

A fully consistent diffuse interface approach to brittle fracture

V. I. Marconi and E. A. Jagla

The Abdus Salam International Centre for Theoretical Physics

Strada Costiera 11, (34014) Trieste, Italy

(February 8, 2020)

We present a continuum model for the propagation of cracks and fractures in brittle materials. The components of the strain tensor ε are the fundamental variables. The evolution equations are based on a free energy that reduces to that of linear elasticity for small ε , and accounts for cracks through energy saturation at large values of ε . We regularize the model by including terms dependent on gradients of ε in the free energy. No additional fields others than the strain tensor ε are introduced, and then the whole dynamics is perfectly defined. We validate the model in controlled cases, and present a couple of non trivial applications.

I. INTRODUCTION

There are many problems in condensed matter physics and materials science in which the aim is to describe sharp interfaces separating regions with qualitatively different properties. This occurs for instance in solidification, dendritic growth, solid-solid transformations, grain growth, etc. Traditionally, two approaches have been followed to tackle these problems. In one of them, the problem is solved including boundary conditions at the interface, and based on this, the expected evolution of the interface in the following time step is calculated, and the process repeated. This method has the practical drawback that the different structure of the interface at each time step makes necessary the full solution of a new problem each time. The second approach is sort of brute force, in which the system is modeled to the atomic scale, and evolved according to their (Newtonian) equations of motion. The problem with this approach is that it is impossible in practice to span the many orders of magnitude between the atomic scale and the relevant macroscopic scale.

The diffuse interface technique (including the so-called phase field models) is a novel powerful approach to study this kind of problems [1]. It typically describes the sharp interface by an additional field ϕ (or more than one). For instance in a solidification problem ϕ can be taken to be 0 in the liquid and 1 in the solid. If the spatial variation of ϕ is known the interface can be located. Then the problem of keep tracking of the interface is eliminated against having to include also ϕ as a new dynamical variable. ϕ is coupled (usually phenomenologically) to the original degrees of freedom of the problem, and its dynamic evolution is not defined *a priori*, but has to be seeded from outside.

A key ingredient in phase field models is *regularization* of the field ϕ . Although the sharp interface is the sensible case, in order to implement the theory a smooth transition of ϕ between the values on both sides of the interface is necessary. Then the interface acquires a fictitious width, which however does not alter the physical

behavior of the system if it is much smaller than any other relevant length scale. An additional, very important effect of regularization is to make the properties of the system independent of the underlying numerical mesh used to implement the problem on the computer. Regularization is usually achieved by the inclusion in the free energy of terms depending on gradients of ϕ , penalizing rapid spatial variations of this quantity.

Within the field of fracture, the phase field models that have been proposed so far include those of Aranson, Kalatsky and Vinokur [2], Karma, Kessler and Levine [3], and Eastgate *et al.* [4] (see also [5]). With some differences, all of them fit well in the previous description. In particular they all include in addition to the elastic variables, the presence of a scalar field ϕ that is taken to be (asymptotically) zero within fractures and one within the intact material. The presence of regularizing terms in the energy of the generic form $\alpha(\nabla\phi)^2$, makes all variables in the system to behave smoothly, and allow to encode the position of the interface in the structure of the field ϕ . Due to the existence of the additional field ϕ , the number of degrees of freedom in the model is larger than in reality. Only in the limit in which $\alpha \rightarrow 0$ the sharp interface limit and the correct number of degrees of freedom is recovered.

The diffuse interface approach we are going to present has a qualitative difference with previous ones. It does not introduce additional variables into the problem, the full set of variables are the components of the strain tensor ε [11]. Description of fracture is achieved by the nonlinear form of the effective free energy density as a function of ε . Actually, our energy is quadratic for small strains (and then correctly describes linear elasticity) and saturates for very large displacements, then describing fracture (the saturation energy value being related to the fracture energy). Regularization is provided by terms in the free energy of the generic form $(\partial\varepsilon)^2$.

Whereas our approach and the previously quoted ones should converge to the same limit in the sharp interface case, we believe ours has a number of advantages, both conceptual and for implementation. Since we do not in-

clude additional degrees of freedom, we do not face the problem of its dynamics. Also, the number of uncontrolled parameters is largely reduced. In our case, our variables ε have all well defined Newtonian dynamics, eventually complemented with some phenomenological damping. From a practical point of view, and in addition to the lower number of degrees of freedom, there is an important difference in the tensorial nature of the variable describing the occurrence of fractures. In the approaches in which a scalar field ϕ is introduced, knowing that ϕ has become zero at some point tells that a fracture is passing through that point, but does not tell anything about what direction the fracture follows. In our case fracture is described by ε itself, and then if we know that a fracture is passing through some point, we can say immediately which direction it has. We believe this is an important computational advantage: a single cell of a computational mesh is sufficient to encode the information about existence and direction of fracture. In models using a scalar field ϕ we need a whole neighborhood of a computational cell to encode the same information.

In some sense our approach could be seen as a generalization of ‘masses and breakable springs’ models. However, the fact that we use the components of the strain tensor as dynamical variables instead of the (vectorial) displacement field is crucial. For instance it allows us to construct a rotationally invariant theory, something very difficult with springs and masses. Also the regularization is a problematic issue in spring and masses models since typically leads to models with derivatives of the displacements up to fourth order, that become cumbersome to treat numerically.

We have divided the presentation in the following form. In section II we present the model. In Section III some validation is presented in well controlled geometries. As an indication of the capabilities of the model we present two particular applications. They are the evolution of two parallel cracks under isotropic loading (Section IV), and the identification of the lowest energy configuration of cracks under a non-homogeneous stress distribution (Section V). In Section VI we summarize our presentation and conclude.

II. THE BASIC MODEL

The fundamental variables of the problem are the components of the strain tensor ε

$$\varepsilon_{ij} \equiv \frac{1}{2} \left(\frac{\partial u_i}{\partial x_j} + \frac{\partial u_j}{\partial x_i} \right) \quad (1)$$

where $u_i(\mathbf{r})$ are the displacements with respect to the unperturbed positions $u_i^0(\mathbf{r})$ [7]. Our approach follows closely that in Ref. [8] (see also [9]) where it was used to study textures in ferroelastic materials and martensites. For clarity we present the model for a two dimensional geometry under plain strain conditions ($u_3(\mathbf{r}) \equiv 0$), the

generalization to three dimensions being conceptually straightforward, although of course more involved. The symmetric tensor ε_{ij} has three independent components. For convenience we will choose them in the form

$$\begin{aligned} e_1 &\equiv (\varepsilon_{11} + \varepsilon_{22})/2 \\ e_2 &\equiv (\varepsilon_{11} - \varepsilon_{22})/2 \\ e_3 &\equiv \varepsilon_{12} = \varepsilon_{21} \end{aligned} \quad (2)$$

which are named respectively the dilation, deviatoric and shear components. These three variables are however not independent. In fact, since ε is derived from the displacements u_i , there is one constraint that has to be fulfilled, leaving only two independent variables. The constraint is known as the St. Venant condition [10], and it can be written as

$$(\partial_x^2 + \partial_y^2)e_1 - (\partial_x^2 - \partial_y^2)e_2 - 2\partial_x\partial_y e_3 = 0. \quad (3)$$

It is easy to show that this is an identity if the definitions (1) and (2) are used [11].

To define the model we need to know the form of the local free energy density $F_L(\varepsilon)$. To correctly describe elasticity for small displacements the limiting form F_L^0 of F_L for small ε should be

$$F_L^0(\varepsilon) = \frac{1}{2} C_{ijkl} \varepsilon_{ij} \varepsilon_{kl} \quad (4)$$

where C_{ijkl} is the fourth order tensor of elastic constants of the material. We will specialize the expressions to an isotropic material, as this was our first aim to use this kind of model. In the isotropic case F_L^0 reads

$$F_L^0(\varepsilon) = B e_1^2 + \mu (e_2^2 + e_3^2) \quad (5)$$

where B and μ are related to the two dimensional bulk and shear modulus. The previous expression of the free energy must be extended to large strains to account for fracture. To do this the energy must saturate for large deformation. This is the main requirement, and different choices can be made. In the simulations presented below for isotropic materials we have chosen

$$F_L(\varepsilon) = \frac{g F_L^0(\varepsilon)}{[1 + F_L^0(\varepsilon)/f_0]} \quad (6)$$

The function $g(\mathbf{r})$ is externally controlled, and may be used to model some random inhomogeneities in the system (when g is chosen to vary randomly, but always being $g \sim 1$) or preexistent cracks in the material (where $g = 0$). The limiting value f_0 of F_L for $\varepsilon \rightarrow \infty$ (assuming $g = 1$), is the energy density necessary to impose locally a very large value for at least one component of ε , and is then related to the crack energy of the problem (see below). From the present free energy form, we see that a crack is nucleating when typical values of e 's are $e_i \sim (f_0/B)^{1/2}$ (assuming $\mu \sim B$).

Experimentally, fracturing implies typically a non-reversible process, in which the material is permanently

damaged once fractured. We note that the description provided by (6) is reversible, in the sense that the system has the possibility of healing the fractures and return to its original configuration if external stresses are relaxed. However, if we are interested in processes in which stresses are applied, and never relaxed, this is not a serious problem, as cracks will not heal (irreversibility can also be phenomenologically included in the model, see Section III-D).

The other crucial ingredient of the model is regularization. That is provided by gradient terms in the free energy density. The terms we have used are of the form

$$F_{gr} = \sum_{i=1,2,3} \alpha_i (\nabla e_i)^2 \quad (7)$$

with numerical coefficients α_i . To retain rotational invariance we have to choose $\alpha_2 = \alpha_3$.

Once the full free energy is defined, the equations of motion are obtained by including a kinetic term T , which is quadratic in temporal derivatives of the displacements (i.e., $T \sim \frac{1}{2} \rho \dot{\mathbf{u}}^2$, for some generic density ρ) and then it has to be transformed to a function of e_1, e_2, e_3 (see [8] for the details). The equations to be solved are more conveniently written in Fourier space (we use E_i for the Fourier transforms of e_i , and $F = F_L + F_{gr}$). The result is

$$\begin{aligned} \frac{4\rho}{k_x^2 k_y^2} (k^2 \ddot{E}_1 + (k_y^2 - k_x^2) \ddot{E}_2) &= -\frac{\partial F}{\partial E_1^*} - A_1 \dot{E}_1 + k^2 \Lambda \\ \frac{4\rho}{k_x^2 k_y^2} ((k_y^2 - k_x^2) \ddot{E}_1 + k^2 \ddot{E}_2) &= -\frac{\partial F}{\partial E_2^*} - A_2 \dot{E}_2 + (k_y^2 - k_x^2) \Lambda \\ 0 &= -\frac{\partial F}{\partial E_3^*} - A_3 \dot{E}_3 - 2k_x k_y \Lambda \end{aligned} \quad (8)$$

where A_1, A_2, A_3 are phenomenological damping coefficients (that we will take always to be equal $A_i \equiv A$) and Λ is a Lagrange multiplier depending implicitly on E 's, chosen to enforce at every moment the St. Venant constraint, that in Fourier space reads

$$(k_x^2 + k_y^2) E_1 - (k_x^2 - k_y^2) E_2 - 2k_x k_y E_3 = 0. \quad (9)$$

In all examples presented below, unless explicitly indicated, we use $\mu = 0.5B$, $f_0 = B$, and the dynamic equations (8) are solved on a 512×512 numerical mesh, using periodic boundary conditions and in the overdamped regime, in which the second order time derivative terms are neglected.

III. VALIDATION OF THE MODEL

We present first different tests of the model in simple and well controlled situations to evaluate its possibilities and limitations.

A. Infinitely long, straight crack

We perform the first analysis in the almost trivial configuration in which a single, straight crack divides an infinite sample in two parts. In this geometry, all quantities depend only on the coordinate x (the crack is assumed to extend along the y direction), and the model becomes effectively one-dimensional. In fact, assuming the boundary conditions impose no strain at infinity in the y direction, we have $e_1(x) = e_2(x)$, $e_3 = 0$. As expected, there is a single order parameter in this configuration, that can be taken to be e_1 . The free energy of the model restricted to the present case (using $g = 1$) becomes simply

$$F/L_y = \int dx \frac{a e_1^2}{1 + (a/f_0) e_1^2} + \frac{\alpha}{2} \int dx |\nabla e_1|^2 \quad (10)$$

where L_y is the system size along the y direction, $\alpha = 2(\alpha_1 + \alpha_2)$ and $a = (B + \mu)$.

A relative stretching $\Delta L_x/L_x$ in the x direction can be imposed by enforcing $\bar{e}_1 = \Delta L_x/L_x$, where the bar denotes the mean value over the system. It is clear that for $\alpha = 0$ the minimum energy solution of the problem has $e_1 = 0$ except at a single point x_0 . The position x_0 is undetermined. This solution describes the system broken at x_0 . The fracture energy per unit length γ in this case is non-zero only if a spatial discretization δ is used. Then $\gamma = f_0 \delta$.

For $\alpha \neq 0$ the situation changes. The free energy (10) can be thought to be the action of a particle of mass α in a potential energy given by minus the integrand of the first term in (10). The sharp fracture of the case $\alpha = 0$ transforms now into a smooth object that occupies a finite width w in the system. Note that w measures the width of the fracture in the *original*, unstrained reference system. A set of numerically obtained curves for $e_1(x)$ for different values of \bar{e}_1 is shown in Fig. 1. The value of e_1 does not go to zero away from the fracture, indicating that there is a remnant stress σ_{rm} in the system. The opening Δ of the fracture is defined as the integral of e_1 across the width of the fracture, namely, it is the area of the peak in Fig. 1. For sufficiently large values of Δ , the following analytic behaviors are obtained: $w \sim (\alpha/f_0)^{1/4} \Delta^{1/2}$, $\sigma_{rm} \sim f_0^{3/4} \alpha^{1/4} \Delta^{-1/2}$. The remnant stress decays to zero upon stretching. This means that fracture tends to be an 'ideal' one for large enough Δ .

Note however that w (and then also the fracture energy γ than now becomes $\gamma \sim f_0 w$) does not saturate for large stretching. This may be problematic for some applications, and we have devised a modification of the model to cure this behavior (note however that in the examples below this modification is not implemented): As the gradient terms are necessary for a fracture to propagate without interference of the numerical mesh, they are only important when fracture is forming, namely, when typical values of e_i are close or lower than $\sim (f_0/B)^{1/2}$. In the regions in which the fracture has nucleated, e 's

become much larger, and the gradient terms are not necessary any more. Then we can weaken their effect in those regions. One way of doing this is multiplying the gradient terms of the free energy by a decreasing function of e_i . We have used the factor $[1 + (\sum_i (e_i/e^*)^2)^n]^{-1}$ multiplying F_{gr} in (7) as a reasonable choice, where e^* is a threshold value, and n controls the sharpness of the cut off. The results with this modification are seen in Fig. 2. Now the fracture is much sharper because most of the elongation is taken over by the central part. However, the external part retains the same smoothed form as before. The thickness w of the fracture saturates for large \bar{e}_1 to a value $w \sim (\alpha/f_0)^{1/2}e^*$, namely fractures never become wider than some fixed value. This produces also a finite and well defined value of the fracture energy $\gamma \sim f_0 w \sim (\alpha f_0)^{1/2}e^*$.

B. Finite straight crack under model I loading

Usually, when fracture problems are solved on an ordered numerical mesh, there is a strong influence of the mesh on the results obtained. The mesh typically produces undesired anisotropy effects that we want to minimize. That is why we will concentrate in the most difficult case from this point of view, namely we want to describe an isotropic material. We already wrote the free energy in the precedent section for this case. To have an isotropic model on a mesh, the discretization of the mesh δ must be smaller than any relevant distance in the system. The smaller relevant distance in the model of the precedent section is the regularized width of the transition between intact parts of the material and fracture. This distance is controlled by the relation between the α_i constants in (7) and the elasticity constants B and μ in (5), and its order of magnitude is $\sim \sqrt{\alpha_i/B}$.

We want to study the evolution of a preexistent rectilinear finite length crack under a slowly increasing remote stress (or strain). We are particularly interested in the critical stress and in the path followed by the crack once it starts propagating. We place in the system cracks of different lengths and at different angles with respect to the numerical mesh, and study their evolution under the application of an isotropic (biaxial) remote strain.

The definition of the preexistent crack is through the function $g(\mathbf{r})$ introduced previously. On the mesh this function becomes g_{ij} , where i, j represent a square element of the mesh. We will consider a crack of length l_0 with one end at point x_0, y_0 at an angle θ with respect to x axis. It is then described by the expressions

$$\begin{aligned} x &= x_0 + \nu \cos(\theta) \\ y &= y_0 + \nu \sin(\theta) \end{aligned} \quad (11)$$

with ν running between 0 and l_0 . We set $g_{ij} = 0$ for all elements such that they are intersected by the crack, as defined by (11). Note that using this definition, the crack length l_0 is the real geometric length, and it is not

necessarily measured by the number of elements on which $g_{ij} = 0$.

The effect of the numerical mesh on crack propagation in the non-regularized model ($\alpha_i = 0$) is particularly strong in the case of biaxial loading. We use this configuration as it will be a much more stringent test of the isotropy of the regularized model than the more common uniaxial loading perpendicular to the crack. Biaxial loading is obtained by taking \bar{e}_1 to be some fixed constant, and $\bar{e}_2 = 0, \bar{e}_3 = 0$. \bar{e}_1 is related to the remote stress σ_0 by $\sigma_0 = B\bar{e}_1$. All results have been obtained using a square numerical mesh, aligned with the x - y coordinate axis.

Basic fracture mechanics [12] tells that the crack should be stable if σ_0 is lower than some critical value σ_c . For an isotropic material, this critical value is of course independent on the angle θ between the crack and the numerical mesh. We calculated in our model σ_c as a function of the angle of the original crack with the x axis, and the results are presented in Fig. 3. For $\alpha_i = 0$, we observe a strong dependence of this value with θ , indicating a spurious anisotropy associated to the numerical mesh. The results for non zero α (we choose the three α_i to be equal to some α) show that σ_c becomes progressively angle independent. In addition, direct examination of the trajectories followed by the crack in both cases (Figs. 4 and 5) shows how in the $\alpha = 0$ case the numerical lattice has an obvious effect onto the crack path. This effect mainly disappears for $\alpha \gtrsim 0.5B\delta^2$, where the crack grows collinearly with its seed. Note the lateral spreading of the crack in the regularized case, as already discussed in the one-dimensional geometry.

C. Non trivial loading. Crack kinking under combined mode I-mode II loading

The mode I loading of the previous section is the simplest case on which we can test our model, and it certainly should be well described by any reasonable model of fracture. We show here that more complex loadings are also well described by the present formalism.

It is known that under combined mode I and mode II loading, an original straight crack propagates in a direction that does not coincide with the original one, namely it kinks [12]. We placed a crack along the x direction, and applied a combination of opening and shear stress, and followed the evolution of the crack. As we can see in Fig. 6, the model reproduces qualitatively the expected behavior of the crack under these conditions. Detailed quantitative comparison will be presented elsewhere.

D. Crack wandering

During our validation calculations we became aware of an unrealistic feature of the regularized model that we

want to discuss now. Once nucleated, and in situations in which they are not stabilized by symmetry, cracks may shift laterally, in addition to extend longitudinally. This wandering originates in the tendency of the cracks to reduce the energy of the system as much as possible. In real situations, this lateral movement of cracks almost never occurs, as it implies the transfer (via diffusion) of material from one face of the crack to the other, and although the final configuration may have a lower energy, the process implies the surmounting of an enormous energy barrier [13]. In our model, the regularization transforms the sharp crack into a smoothed one, and we can understand the movement by doing the analogy with dislocations in the Frenkel-Kontorova model [14]: when they are sharp they are pinned, but when they are extended objects they find much lower energy barriers to move. We have actually seen in some simulations how cracks move laterally in order to minimize the energy of the system. However, in the simulations of the preceding sections this movement was almost unnoticeable in the time scales we have considered. But we have seen the effect to occur in longer time-scales. This drift should be considered a drawback of the model [15] (see however Section V).

A direct approach that can be implemented to avoid this problem is to take account in an effective way of the irreversible process occurring in a real system during fracture (for instance, oxidation of the crack faces). A very simple way of doing this is to prescribe that when the value of e_1 at some point exceeds some fixed value (chosen in the range in which we can assure the crack has been nucleated at that point) the function g is set to zero at that point and for ever (in this way we are introducing an effective irreversibility in the model). This will produce a strong tendency for the crack to remain there and not to move laterally, as now it does not pay any energy to be there. In other words, the crack remains ‘pinned’ to the sites where $g = 0$. This trick has proved to be enough to avoid crack wandering in all cases in which we have observed it to be noticeable.

IV. EFFECTS OF ELASTIC INTERACTION BETWEEN CRACKS

The prediction of crack trajectories under general crack-loading conditions is very important in many engineering applications. The present formalism is well suited to study this kind of problems, in particular in those cases in which slight deviations from straight propagation are expected. These cases are particularly difficult to tackle with a non-regularized model. As a very simple illustrative example of that, we consider a pair of parallel cracks. We show here some results very briefly, leaving a more detailed quantitative analysis for a forthcoming work. We follow the evolution of the system upon the application of a finite isotropic strain. Snapshots of the system during crack propagation (Fig. 7) shows that although the loading is isotropic, the cracks diverge from

each other during propagation. This is a non-trivial effect caused by the elastic interaction between the two cracks. Note that in the present case, cracks propagate from *both* fractures, because of the perfect mirror symmetry of the problem with respect to the middle plane. If this symmetry is broken (for instance making one crack larger than the other, or introducing some random inhomogeneities), we have observed only one crack propagating, as in fact occurs in experiments.

V. IDEAL CRACK CONFIGURATION UNDER NON-HOMOGENEOUS LOADING

Although we have seen that the lateral wandering of cracks is typically an undesirable effect in the model, this may not be so in certain cases. Those include the cases in which we are interested precisely in determining the configuration of cracks that minimizes the total energy of the system. We provide one example here. Let us suppose that a two dimensional uniform and isotropic material is cooled in a circular region. This cooling generates a contraction in that part of the material, and if it is strong enough it may produce the appearance of some cracks. What is the configuration of cracks such that the sum of the elastic energy of the system and the crack energy is minimized? This problem can be tackled straightforwardly with the present model. Actually, the lateral wandering of cracks will now be a helpful characteristic, since the system adapts itself to find the lowest energy configuration.

To solve this problem we modified the equations of motion including a fluctuation term in the standard Langevin form [16]. This term enhances the wandering of cracks, then permitting to perform an annealing process to find the lowest energy of the system. The effect of external temperature is considered to change the preferred local values of the density of the system, or equivalently the preferred values of e_1 . To model this, we modified the free energy density (5) to the new expression

$$F_L^0(\varepsilon) = B(e_1 - e_1^0(\mathbf{r}))^2 + \mu(e_2^2 + e_3^2) \quad (12)$$

where $e_i^0(\mathbf{r})$ are fixed external functions that allow to prescribe the strain configuration locally preferred by the system. We use a function $e_1^0(\mathbf{r})$ that reflects the effect of external temperature onto the system. We have obtained the crack configurations that minimize the energy under two different form of the $e_1^0(\mathbf{r})$ function: in one case e_1^0 is a constant $k < 0$ inside a circle of radius $R = 50\delta$, and zero outside. In the second case the transition is gradual, and the value of e_1^0 as a function of the distance r from the center is given by $e_1^0(r) = k \exp(-r^2/R^2)$. Results are presented in Fig. 8, and are seen to be qualitatively different in both cases. For the sharp temperature profile, a circular crack extending along most (although not all) of the circle $r = R$ minimizes the energy. For the Gaussian profile, a triple junction at the center of the circle provides the best solution.

VI. SUMMARY, OUTLOOK AND CONCLUSIONS.

In summary, we have presented a model for the study of cracks propagating in brittle materials. The model does not use additional variables other than the strain tensor, and then is well defined once the free energy is defined. As a crucial ingredient it includes regularization terms that make the cracks to be smoothed. We have shown that in this form our model can describe accurately an isotropic material in conditions in which the non-regularized model fails neatly. We have seen that given the possibility of doing simulations in sufficiently large numerical meshes, the cracks can be defined to any necessary precision.

The validation and applications have been presented very briefly, in order to give an overall view of the possibilities of the technique. They have included the extension of crack under simple mode I, and combined mode I-mode II conditions, the study of non-trivial effects due to crack-crack interaction, and the determination of minimum energy configurations of cracks. Although we have presented only examples on quasistatic crack propagation, the equations of the model have been presented in its general form including the kinetic energy of the material. This allows the model to be used to study problems in dynamic fracture mechanics, such as crack instabilities and bifurcation, sound emission, etc.

We believe that the present technique is straightforward to implement and computationally efficient, and that it addresses in a phenomenological way the very important applied problem of predicting crack evolution, without requiring to know details about the physical conditions in the process zone. The technique can be used also in three dimensions, although we feel that this should wait for some increase in computational power before it can be implemented on a desktop computer.

VII. ACKNOWLEDGMENTS

We thank S. R. Shenoy for comments and discussions.

-
- [1] H. Emmerich, *The diffuse Interface Approach in Condensed Matter*, (Springer, Berlin, 2003); L.-Q. Chen, *Annu. Rev. Mater. Sci.* **32**, 113 (2002).
 - [2] I. S. Aranson, V. A. Kalatsky, and V. M. Vinokur, *Phys. Rev. Lett.* **85**, 118 (2000).
 - [3] A. Karma, D. A. Kessler, and H. Levine, *Phys. Rev. Lett.* **87**, 045501 (2001).
 - [4] L. O. Eastgate, J. P. Sethna, M. Rauscher, T. Cretegny, C.-S. Chen, and C. R. Myers, *Phys. Rev. E* **65**, 036117 (2002).

- [5] The theory presented by Y. M. Jin, Y. U. Wang, and A. G. Khachaturyan [*Philos. Mag.* **83**, 1587 (2003)] uses a phase field of tensorial nature, and then is close to the one we present here. However, it seems to be applicable only when there is a finite number of cleavage planes in the material.
- [6] That is why we prefer to call our approach a diffuse interface one. We reserve the term 'phase field model' for cases where there are additional fields.
- [7] We do not include at present the non-linear part of the strain tensor ($\sim \frac{\partial u_k}{\partial x_i} \frac{\partial u_k}{\partial x_j}$), and then in its present form our formalism does not properly describe problems in which finite relative rotations of different parts of the body occur.
- [8] T. Lookman, S. R. Shenoy, K. O. Rasmussen, A. Saxena, and A. R. Bishop, *Phys. Rev. B* **67**, 024114 (2003); S. R. Shenoy, T. Lookman, A. Saxena, and A. R. Bishop, *Phys. Rev. B* **60**, R12537 (1999).
- [9] S. Kartha, J. A. Krumhansl, J. P. Sethna, and L. K. Wickham, *Phys. Rev. B* **52**, 803 (1995).
- [10] D. S. Chandrasekharaiiah and L. Debnath, *Continuum Mechanics*, (Academic, San Diego, 1996).
- [11] We prefer to work in terms of the three variables e_1 , e_2 , and e_3 , and enforce the compatibility condition by using a Lagrange multiplier. Notwithstanding, it should be mentioned that another possibility is to use only two truly independent variables, expressing explicitly the third one in terms of the other two using the compatibility equation (3). In that case we would obtain a non-local, long range interaction between the two independent variables, as explained in Refs. [8] and [9].
- [12] K. B. Broberg, *Cracks and Fracture*, (Academic, San Diego, 1999).
- [13] E. A. Brener and V. I Marchenko, *Phys. Rev. Lett.* **81**, 5141 (1998); R. Spatschek and E. A. Brener, *Phys. Rev. E* **64**, 046120 (2001).
- [14] P. M. Chaikin and T. C. Lubensky, *Principles of Condensed Matter Physics*, (University Press, Cambridge, 1995).
- [15] This problem should appear also in the others phase field models of fracture [2,3,4,5].
- [16] W. T. Coffey, Y. P. Kalmykov, and J. T. Waldron, *The Langevin Equation*, (World Scientific, Singapore, 1996).

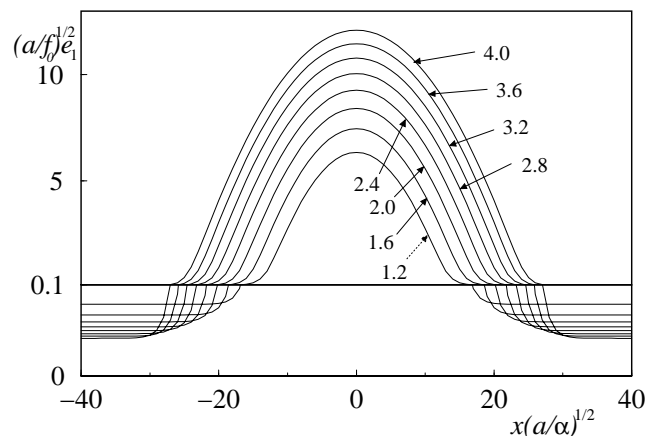


FIG. 1. Profiles of e_1 for the one-dimensional problem, at different values of the global strain $\bar{e}_1 = \delta L_x / L_x$. Labels are the values of $(a/f_0)^{1/2} \bar{e}_1$ used for each curve. Note that e_1 does not go to zero away from the fracture, but a remnant strain remains. This value however, decreases when the fracture is opened wider.

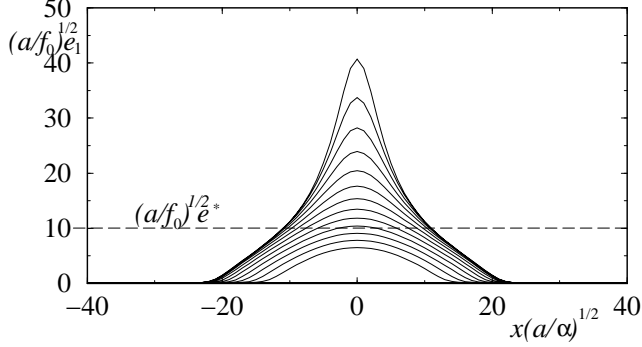


FIG. 2. Modified profiles of e_1 for the one-dimensional problem when the gradient terms are cut off at large values of e_i , as explained in the text. Parameters used are $e^* = 10(a/f_0)^{-1/2}$, $n = 2$. Note that contrary to the case in the previous figure, the fracture width (and this implies also the fracture energy) saturates to a finite value for large \bar{e}_1 .

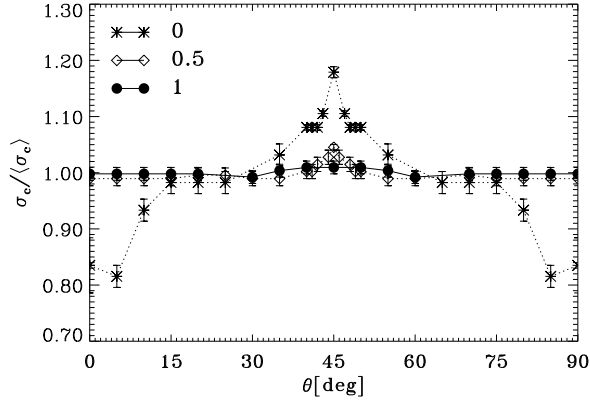


FIG. 3. Critical remote stress σ_c for different values of $\alpha' \equiv \alpha/B\delta^2$ (as indicated), normalized by the mean values, $\langle \sigma_c \rangle = 0.2B$ (for $\alpha' = 0$), $\langle \sigma_c \rangle = 0.79B$ ($\alpha' = 0.5$), $\langle \sigma_c \rangle = 0.88B$ ($\alpha' = 1$). for the propagation of cracks of length $l_0 = 16\delta$ placed at different angles with respect to the numerical mesh. The strong dependence with angle in the $\alpha = 0$ case becomes weaker after the inclusion of the regularization.

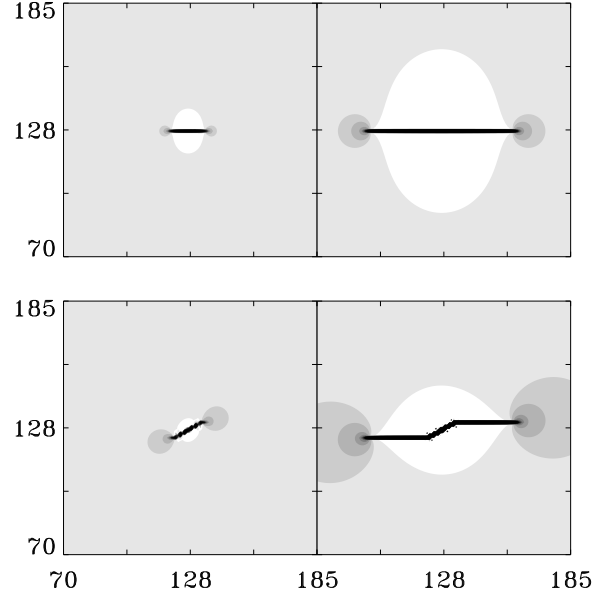


FIG. 4. Snapshots of cracks of original length $l_0 = 16\delta$ growing with $\theta = 0$ deg (upper plots), and $\theta = 30$ deg (lower plots) for $\alpha = 0$ and a remote isotropic strain $\bar{e}_1 = 0.19$, larger than the corresponding critical value. The left panels are the configuration soon after the application of the loading, and the right panels are those some time later. The influence of the numerical mesh is evident. The simulations were done in a system of size 256×256 , and the spatial coordinates are in units of the mesh discretization δ . The key to the gray scale here and in all following figures is as follows: We plot in gray scale the values of e_1 from white (lowest e_1) to black for a value $e_1 \gtrsim 1$ (corresponding to the crossover to cracked material). All values above that one are also plotted black and correspond to the inside crack region.

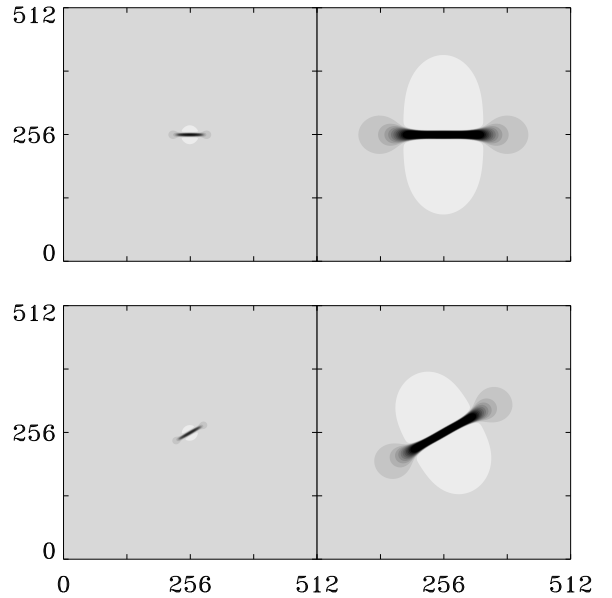


FIG. 5. Same as previous figure for $\alpha = 0.25B\delta^2$, $l_0 = 48\delta$ and $\bar{e}_1 = 0.5$. The effect of the numerical mesh is undetectable.

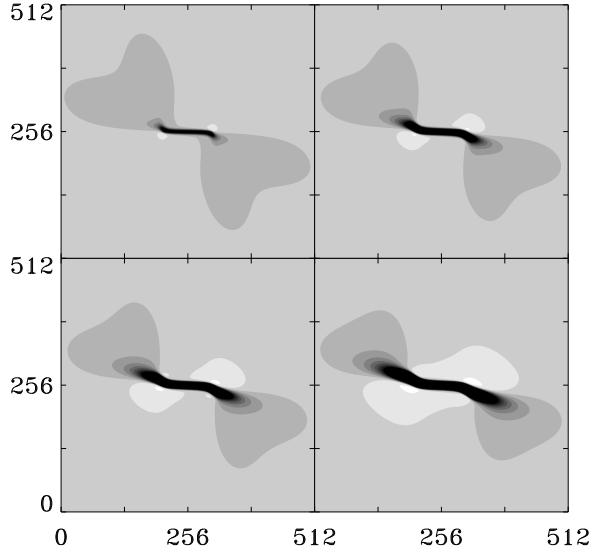


FIG. 6. Time sequence for a horizontal crack ($l_0 = 100\delta$) with $\alpha = 0.5B\delta^2$ growing under combined application of mode I and mode II loads, obtained by taking: $\bar{e}_1 = 0.3$, $\bar{e}_2 = 0$, $\bar{e}_3 = 0.6$. This correspond to a uniaxial stress applied on the diagonal of the system, along the top-right/bottom-left direction.

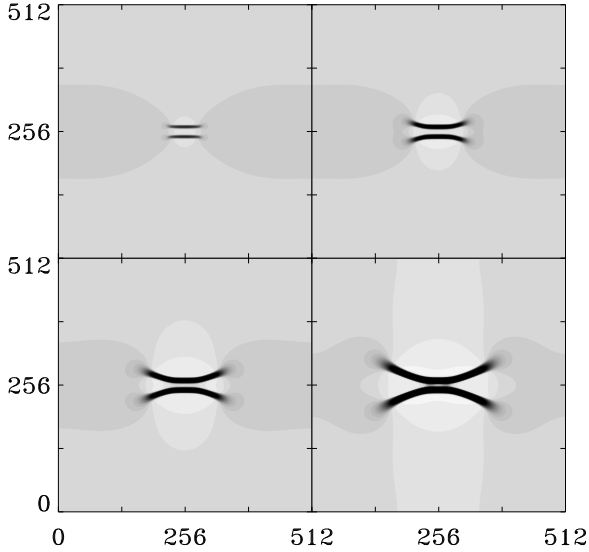


FIG. 7. Time sequence for two parallel cracks (length $l_0 = 60\delta$, separation equal to 20δ) loaded isotropically under $\bar{e}_1=0.5$ (with $\alpha = 0.25B\delta^2$). The cracks extend with some divergence, due to a non-trivial effect of elastic interaction between the two.

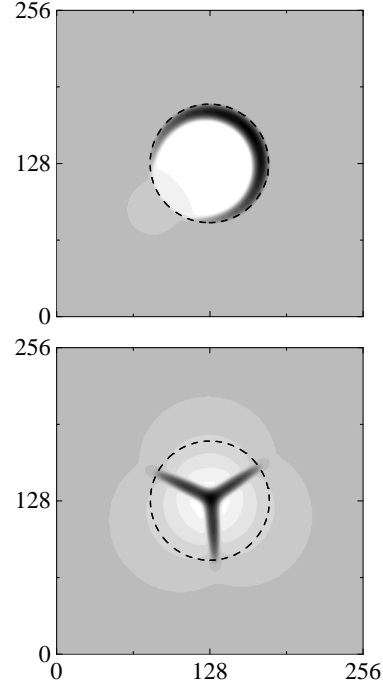


FIG. 8. Crack configurations that minimize the energy of the system when a region is assumed to have a lower preferred value of e_1 . The nominal preferred value of e_1 is $e_1^0(r) = -\theta(-R-r)$ for the upper plot (θ is the Heaviside function), and $e_1^0(r) = -\exp(-r^2/R^2)$ for the lower plot, where r is the distance from the center of the figure and $R = 50\delta$ is the radius of the circle indicated by the dotted lines. Parameters used are: $\mu = 0.5B$, $\alpha = 0.5B\delta^2$, $f_0 = 0.5B$, simulations done in a 256×256 system.